RSC Advances

PAPER

View Article Online
View Journal | View Issue

Cite this: *RSC Adv.*, 2022, **12**, 23169

A carboxylated cellulose aerogel for the rapid detection of aniline vapor†

Luyu Wang, [a] Bing Wang*[a] and Jia Song[b]

Although many aniline vapor sensing materials have superior properties based on the quartz crystal microbalance (QCM) platform, they exhibit very slow response. Herein, we report an effective method to evenly synthesize carboxylated cellulose aerogels *via* 2,2,6,6-tetramethylpiperidine-1-oxy radical (TEMPO)-mediated oxidation. The carboxylated cellulose aerogel was first employed to detect aniline vapor based on a QCM and featured a high response, good selectivity, satisfactory repeatability and stability, and especially rapid response (the response/recovery times were 13 s/8 s, respectively). The Gaussian 09 software was used to simulate the sensing mechanism, which revealed that the weak chemical adsorption between the carboxyl group in the carboxylated cellulose aerogel and the amino group in aniline is the main interaction. These systematic studies show that the carboxylated cellulose aerogel is expected to be a good sensing material for detecting aniline vapor indoors and outdoors.

Received 13th June 2022
Accepted 3rd August 2022

DOI: 10.1039/d2ra03641j

rsc.li/rsc-advances

1. Introduction

Aniline is a carcinogen that has adverse effects on human health, causing chronic poisoning and damage to the liver, kidney and skin.[1] Aniline is also widely used as an accelerator for the vulcanization of dyes, resins, and rubbers.[2] Therefore, the development of an aniline sensing system is urgently required. A variety of analytical methods have been reported for the determination of aniline, including spectrophotometry,[3] chromatography,[4] and electrochemical methods.[5] However, these methods are complex and time-consuming. In contrast, chemical sensors are widely used because of their simplicity,[6] and so it is necessary to develop gas sensors that can quickly detect aniline vapor.

A gas sensor is a kind of device that can detect a variety of target gases in real-time.[7] Due to the need for reducing power consumption, quartz crystal microbalances (QCMs) operating at room temperature have recently attracted wide attention in the field of gas sensors.[8] By developing different sensitizing materials, QCMs can be endowed with diverse gas targeting and sensing performances.[9] For example, hydroxyl-containing $Cu(OH)_2$ nanowires are used to detect humidity,[10] fluoroalcohol-functionalized SBA-15 is used to detect dimethyl methyl phosphonate,[11] *etc.*

Similarly, many sensing materials are designed and coated with QCMs to detect aniline vapor, including UIO-66,[12] hydroxyapatite,[13] and carbon nanocage-embedded nanofibers.[14] The sensitivity, selectivity and stability of these sensors to aniline vapor are satisfactory, but their response and recovery take several minutes. It is obvious that a long response time is not conducive to timely alarms, and a long recovery time is not conducive to reusing the sensor.[15] Therefore, it is necessary to develop novel aniline sensing materials with rapid response/recovery.

As a novel kind of adsorption material, aerogel has the advantages of light weight, high porosity, high surface area, and low density compared with other traditional porous materials.[16,17] These advantages are important for the QCM platform based on adsorption to achieve sensing capabilities.[18,19] Herein, we designed a QCM sensor based on carboxylated cellulose

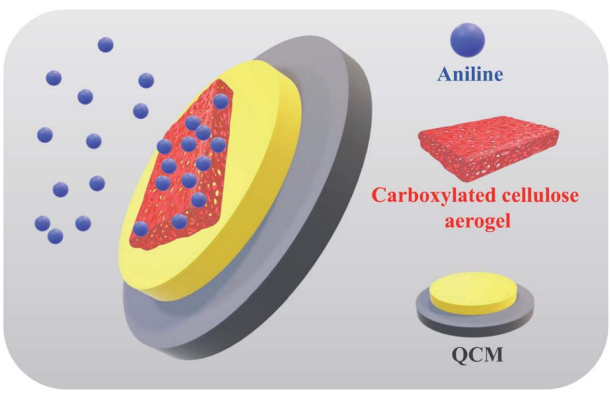

Fig. 1 Scheme of the present experiment.

[a]*College of Artificial Intelligence and E-Commerce, Zhejiang Gongshang University Hangzhou College of Commerce, Hangzhou, 311599, China. E-mail: Dr. Luyu-Wang@hotmail.com; iceking0706@zjgsu.edu.cn*

[b]*School of Nuclear Science and Engineering, Shanghai Jiao Tong University, Shanghai, 200240, China*

† Electronic supplementary information (ESI) available: Synthetic information; characterization process; sensor fabrication information; schematic of the testing system; Gaussian calculations. See https://doi.org/10.1039/d2ra03641j

aerogel for the rapid detection of aniline vapor, as shown in Fig. 1. The response and recovery times are 13 s and 8 s, respectively. This should be attributed to the abundant pore structure of the aerogel,[20] which is conducive to enhancing the speed of aniline molecules in and out. The sensitivity, selectivity and stability of this sensor are also superior. Simulated calculations based on the Gaussian 09 software show that the carboxyl groups in the structure of the carboxylated cellulose aerogel play a key role.

2. Experimental section

2.1. Materials

2,2,6,6-Tetramethylpiperidine-1-oxy and methylene blue were obtained from Alfa Aesar. All the other reagents were purchased from Sinopharm Chemical Reagent Co. Ltd. QCM resonators with silver electrode were purchased from Chengdu Westsensor Co., China.

2.2. Synthesis of the carboxylated cellulose aerogel

The processes of synthesizing the carboxylated cellulose aerogel are displayed in the ESI.† Fig. 2 shows the schematic process of the TEMPO oxidation of the cellulose aerogel. The carboxylated cellulose aerogels with different sodium hypochlorite addition amounts (1, 3, 5, and 7 mmol g^{-1}) were named CA-C-1, CA-C-3, CA-C-5, and CA-C-7, respectively.

2.3. Characterization

The characterization instruments and methods of the above materials are shown in the ESI.†

2.4. Fabrication and test methods of the QCM sensor

The fabrication and test methods of the sensor are obtained from a previous report and are described in detail in the ESI.†[21] Fig. S1† in the ESI shows a schematic of the testing system.

2.5. Gaussian calculations

Based on a previous report,[22] we explored the sensing mechanism *via* simulation calculations and described the relevant parameters in detail in the ESI.†

3. Results and discussion

3.1. Material characterization

Fig. 3a shows an SEM image of CA-C-1. The image shows abundant pore structures with pore sizes ranging from 10 μm to 100 μm. The fibers in some areas have built plates or flocks or flat ribbons. The infrared spectrum of CA-C-1 is shown in Fig. 3b. The vibration peaks appear at 3411.02 cm^{-1}, 2919.26 cm^{-1} and 1434.82 cm^{-1}, corresponding to the stretching vibrations of the –OH, C–H and C–O groups. Besides, the carboxylated cellulose aerogel has a vibration peak at 1630.35 cm^{-1}, which belongs to the stretching vibration of the carboxylate group.[23] In conclusion, the carboxylation reaction takes place on cellulose, in which the hydroxymethyl part is transformed into a carboxylate group.

Fig. 4a shows the carboxyl content of the carboxylated cellulose aerogels prepared with different addition amounts of sodium hypochlorite. In the process of the TEMPO-mediated oxidation of cellulose, the content of carboxyl groups was mainly affected by the addition amount of sodium hypochlorite. As shown in Fig. 4a, the content of carboxyl groups increases with the increase in the amount of sodium hypochlorite added. Therefore, the carboxyl content of the carboxylated cellulose aerogels we synthesized is in the order of CA-C-7 > CA-C-5 > CA-

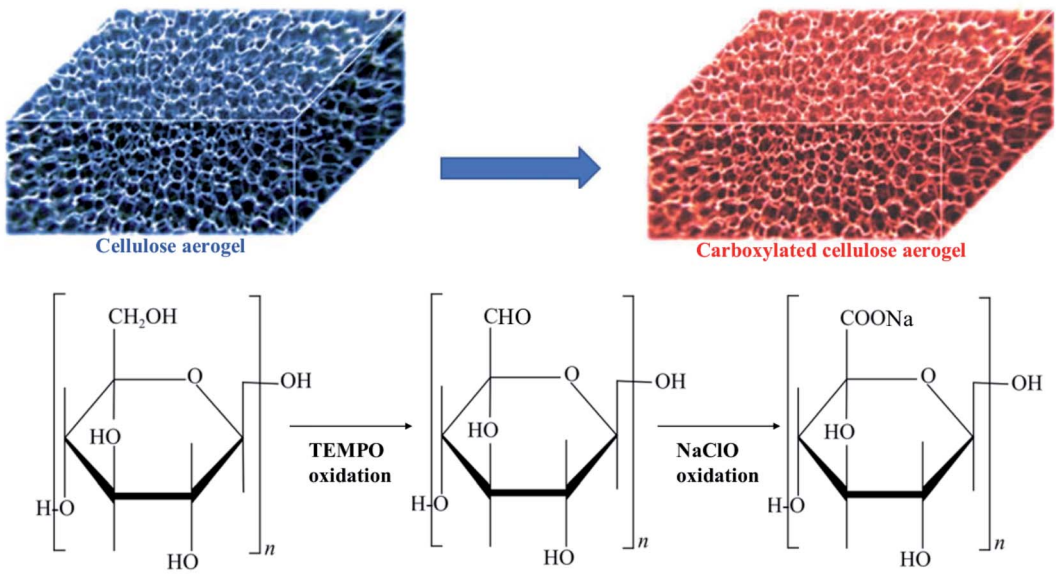

Fig. 2 Schematic process of the TEMPO oxidation of the cellulose aerogel.

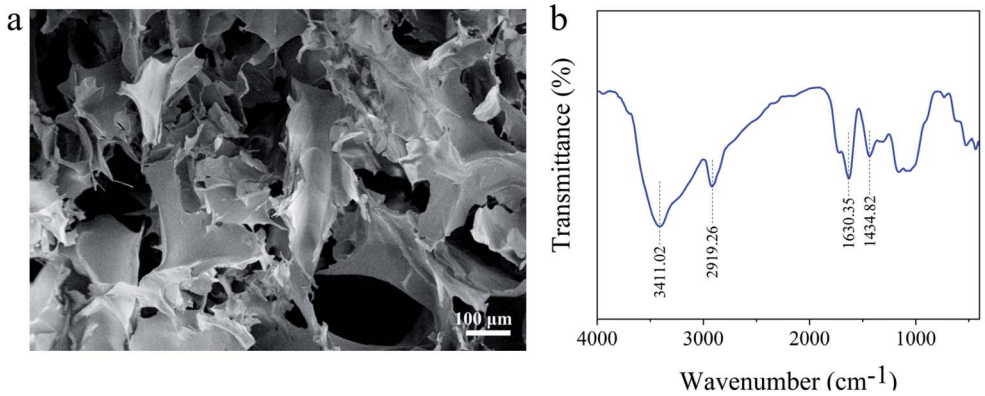

Fig. 3 (a) SEM image of the TEMPO-oxidized cellulose aerogel. (b) FT-IR spectrum of the TEMPO-oxidized cellulose aerogel.

C-3 > CA-C-1. This should be attributed to the continuous enhancement of the carboxylation reaction. Fig. 4b shows the porosity of the carboxylated cellulose aerogels with different sodium hypochlorite addition amounts. The porosity of the carboxylated cellulose aerogels we synthesized is in the order of CA-C-3 > CA-C-5 > CA-C-1 > CA-C-7. The carboxylated cellulose aerogels have high porosity with a maximum value of 87%, which should be attributed to their regular three-dimensional pore structure. However, excessive addition of sodium hypochlorite (7 mmol g^{-1}) leads to excessive carboxylation of the cellulose aerogel, and the porosity tends to decrease instead.

3.2. Sensing properties

Fig. 5a presents the frequency response of six kinds of QCM sensors based on various sensing layers, including pristine QCM, cellulose aerogel (CA), and the four kinds of carboxylated cellulose aerogels (CA-C-1, CA-C-3, CA-C-5, and CA-C-7) towards 1, 10, 20, 30 and 40 ppm aniline vapor at 298 K (ppm represents parts per million in volume). It can be clearly observed that the CA-C-5-based QCM sensor exhibits an obviously larger response under various concentrations of aniline vapor. This should be attributed to the high carboxylic content and porosity of CA-C-5, as shown in Fig. 4. Abundant carboxylic sites provide plenty of reactive sites for the amino groups in aniline molecules, and high porosity allows more aniline molecules to pass through. Therefore, CA-C-5 was selected as the optimal QCM sensing layer for further research.

The real-time sensing curve in Fig. 5b records the response of the CA-C-5-based QCM sensor with the concentration of aniline vapor in the range of 1 to 40 ppm. The limit of detection of the CA-C-5-based QCM sensor for aniline vapor is lower than 1 ppm. This real-time sensing curve can be further transformed into an isotherm, as shown in Fig. 5c. The relationship of the response *versus* the concentration of aniline vapor was explored by fitting. The fitting function is calculated to be $y = 7.17x + 1.25$ for the CA-C-5-based QCM sensor. The corresponding correlation coefficient (R^2) is 0.9986. Clearly, the CA-C-5-based QCM sensor possesses linearity towards aniline vapor concentration. Fig. 5d exhibits the response/recovery curve of the CA-C-5-based QCM sensor exposed to 1 ppm aniline vapor. The result shows that the response and recovery times of the CA-C-5-based QCM sensor towards aniline vapor are about 13 and 8 s, respectively. The response and recovery times of the CA-C-5-based QCM sensor are excellent. Table 1 lists the response and recovery

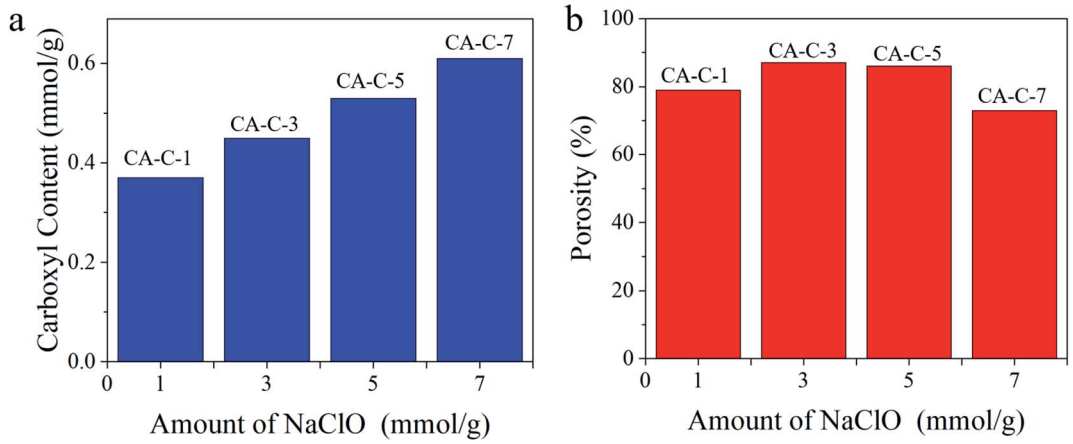

Fig. 4 (a) Carboxyl content of the carboxylated cellulose aerogels prepared with different NaClO addition amounts. (b) Porosity of the carboxylated cellulose aerogels prepared with different NaClO addition amounts.

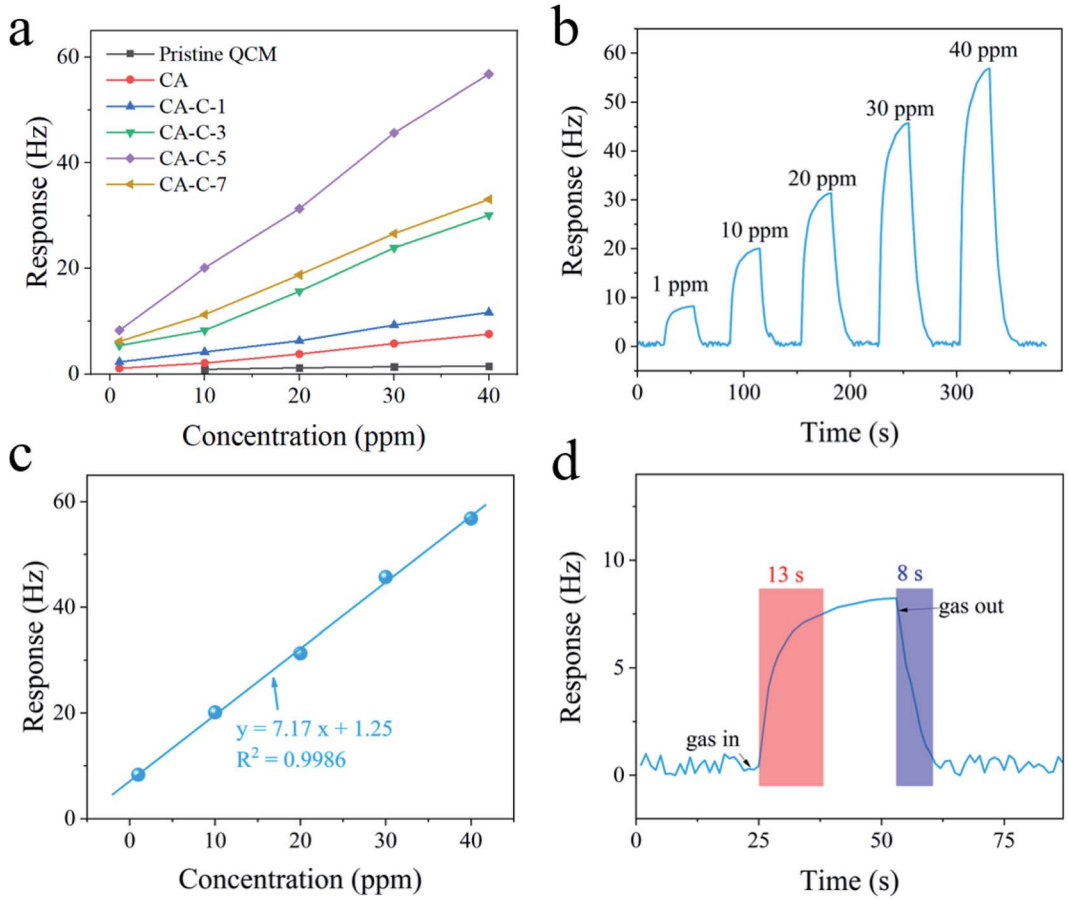

Fig. 5 (a) Response of six kinds of QCM-based sensors to 1–40 ppm aniline vapor at 298 K. (b) Dynamic response curve of the CA-C-5-based QCM sensor when exposed to aniline vapor from low to high concentration at 298 K. (c) Fitting curve of the correlation function between response and aniline concentration. (d) Typical response/recovery curve of the CA-C-5-based QCM sensor to 1 ppm aniline vapor at 298 K.

times of some aniline sensing materials (including CA-C-5 from this work) based on the QCM platform. The response and recovery times of these reported aniline sensing materials are more than 60 s. In contrast, the response time (13 s) and recovery time (8 s) of the CA-C-5-based QCM sensor show its rapid sensing ability.

Repeatability is a significant performance index of gas sensors.[24] Fig. 6a shows the repeatability test result of the CA-C-5-based QCM sensor for 40 ppm aniline vapor at 298 K. The sensor was exposed to 40 ppm aniline vapor and flushed with pure air for three successive cycles. The response under the same exposure concentration is almost unchanged, which shows the favorable repeatability of the CA-C-5-based QCM sensor. As shown in Fig. 6b, five different vapor concentrations (1, 10, 20, 30 and 40 ppm) were selected to test the long-term stability of the CA-C-5-based QCM sensor at 298 K within 30 days. The response fluctuation of the CA-C-5-based QCM sensor under the same concentration is very small, indicating its excellent long-term stability.

Fig. 7a depicts the response of the CA-C-5-based QCM sensor to 30 ppm aniline vapor under a test environment of 40–95% RH. As the relative humidity increases, the response to aniline vapor increases from 39.2 Hz at 40% RH to 65.7 Hz at 95% RH. Environmental humidity plays a role in the detection of aniline

Table 1 Comparison between reported aniline sensing materials and this work

Material	Response time	Recovery time	Reference
UIO-66-$(OH)_2$	135 s	74 s	12
Hydroxyapatite	151 s	778 s	13
Carbon nanocage-embedded nanofiber	>300 s	—	14
CA-C-5	13 s	8 s	This work

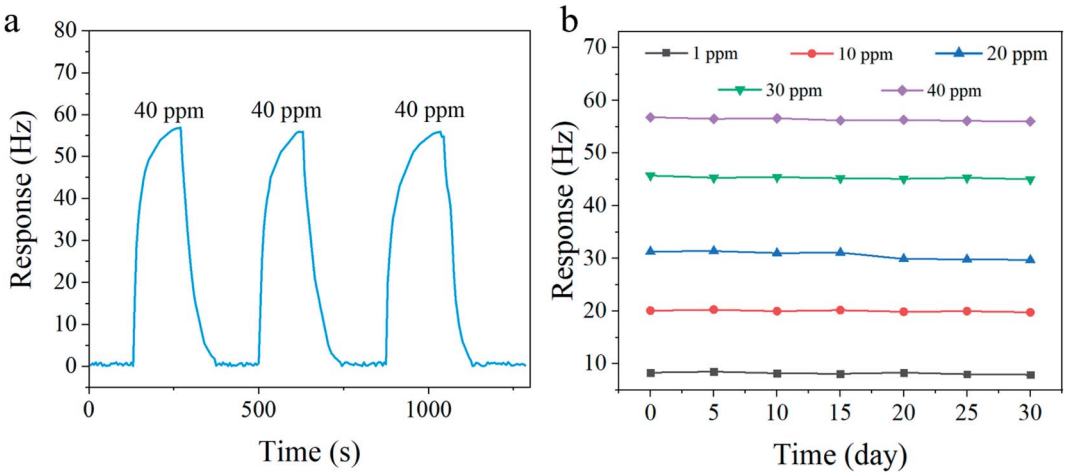

Fig. 6 (a) Continuous repeatability test and (b) long-term stability test of the CA-C-5-based QCM sensor to aniline vapor at 298 K.

vapor using the CA-C-5-based sensor. This phenomenon should be attributed to the cellulose in the sensing material, which can adsorb water molecules from the air in high-humidity environments because of the presence of hydrophilic hydroxyl groups. The additional adsorbed water molecules increase the adsorption mass and reduce the fundamental frequency of the CA-C-5-based QCM sensor.[25] When aniline vapor is introduced, aniline is adsorbed by the sensing material. Moreover, the amino groups in aniline interact with the additional absorbed water molecules through weak hydrogen bonds, which

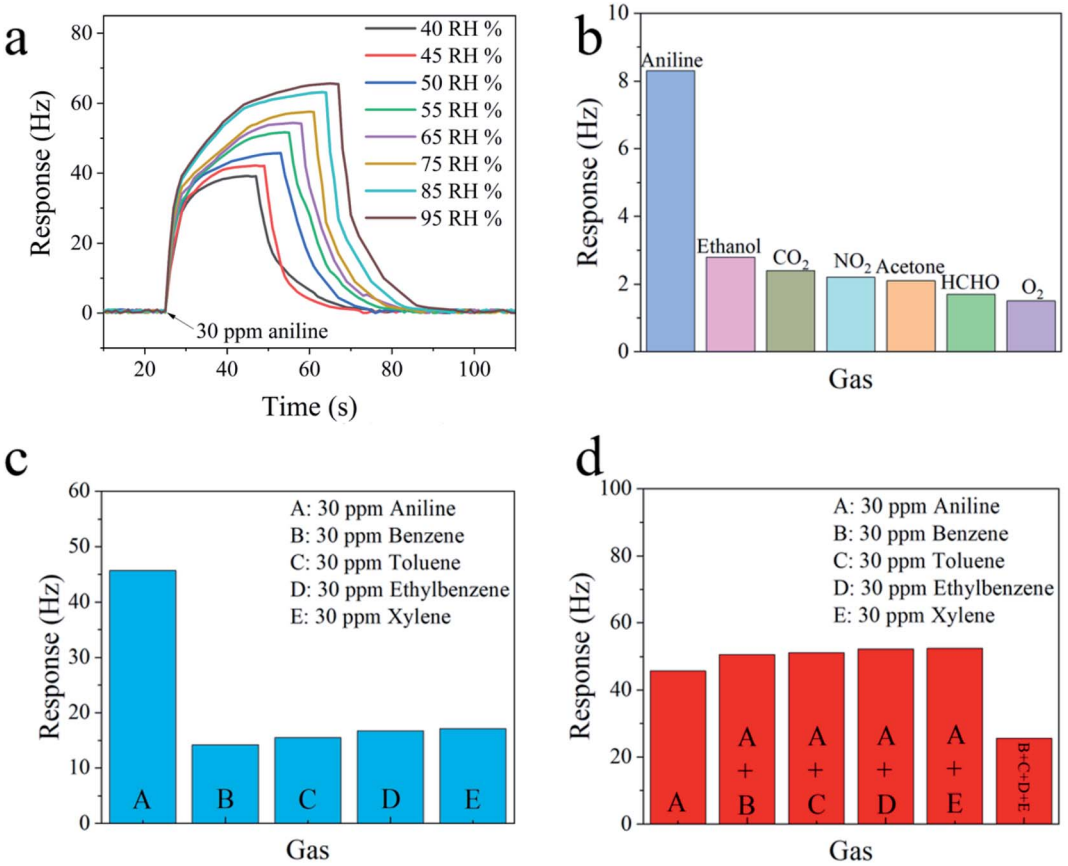

Fig. 7 (a) Response of the CA-C-5-based QCM sensor to 30 ppm aniline vapor under different relative humidity conditions at 298 K. (b) Selectivity tests of the CA-C-5-based QCM sensor to 1 ppm of various gases at 298 K. (c) Comparison of the response of the CA-C-5-based QCM sensor to five kinds of vapor (the concentration of all vapors is set to 30 ppm). (d) Response data showing the selectivity of the CA-C-5-based QCM sensor when exposed to aniline and interferent BTEX vapors with a concentration of 30 ppm.

enhances the physical adsorption of aniline. Therefore, it is expected to utilize post-processing, such as computational error compensation, to enhance the accuracy of the actual aniline sensing measurement in the future.

The selectivity of the CA-C-5-based QCM sensor was evaluated by exposure to 1 ppm of various interferent gases at 298 K, including ethanol, CO_2, NO_2, acetone, HCHO, and O_2, as shown in Fig. 7b. The response of this sensor to aniline vapor is significantly higher than that to other gases.

During the process of aniline vapor detection, it is important to improve the anti-interference ability of BTEX vapors, *i.e.* benzene, toluene, ethylbenzene, and xylene vapors.[26] We compared the sensing performances towards aniline vapor and BTEX vapors of the CA-C-5-based QCM sensor. The concentration of the five vapors was uniformly set at 30 ppm. As shown in Fig. 7c, the responses of the CA-C-5-based QCM sensor to aniline vapor, benzene vapor, toluene vapor, ethylbenzene vapor, and xylene vapor are 45.7 Hz, 14.2 Hz, 15.5 Hz, 16.7 Hz and 17.1 Hz, respectively, indicating the selective detection ability of the CA-C-5-based QCM sensor to aniline vapor against BTEX vapors. This should be attributed to the oxygenated functional groups of CA-C-5, which can introduce hydrogen bond adsorption with the $-NH_2$ group in the aniline structure.

Further, the CA-C-5-based QCM sensor was exposed to aniline vapor mixed with four interfering BTEX vapors, namely benzene vapor, toluene vapor, ethylbenzene vapor, and xylene vapor, to further assess its practical selectivity. The concentration of all the five vapor systems was uniformly set at 30 ppm. The corresponding response data are listed in Fig. 7d. It should be noted that after we introduced other vapors to aniline vapor, although the response increased, the increase was not significant, demonstrating the excellent selectivity of this sensor against various interfering BTEX mixtures. Besides, the response to the four interfering BTEX vapor mixtures (25.5 Hz) is much lower than that of aniline vapor (45.7 Hz). The above results show that the CA-C-5-based QCM aniline sensor has the advantage of resistance to BTEX vapors.

3.3. Sensing mechanism

Exploring the interaction mode between gas molecules and the functional group of the sensing material is an efficient way to obtain the sensing mechanism.[27] However, there are many different groups in the carboxylated cellulose aerogel. It is hard to use experimental methods to explore their roles in the aniline sensing process. Therefore, we used simulation calculations to carry out the related exploration. Li and coworkers[23] reported the molecular formula of carboxylated cellulose obtained after the carboxylation of cellulose with TEMPO. The corresponding monomer molecular structure is used for the simulation calculations using the Gaussian 09 software. First, hydrogen bond adsorption can occur between the oxygen atom of the carboxyl group and the hydrogen atom of aniline. Additionally, the hydroxyl group of carboxylated cellulose can absorb the

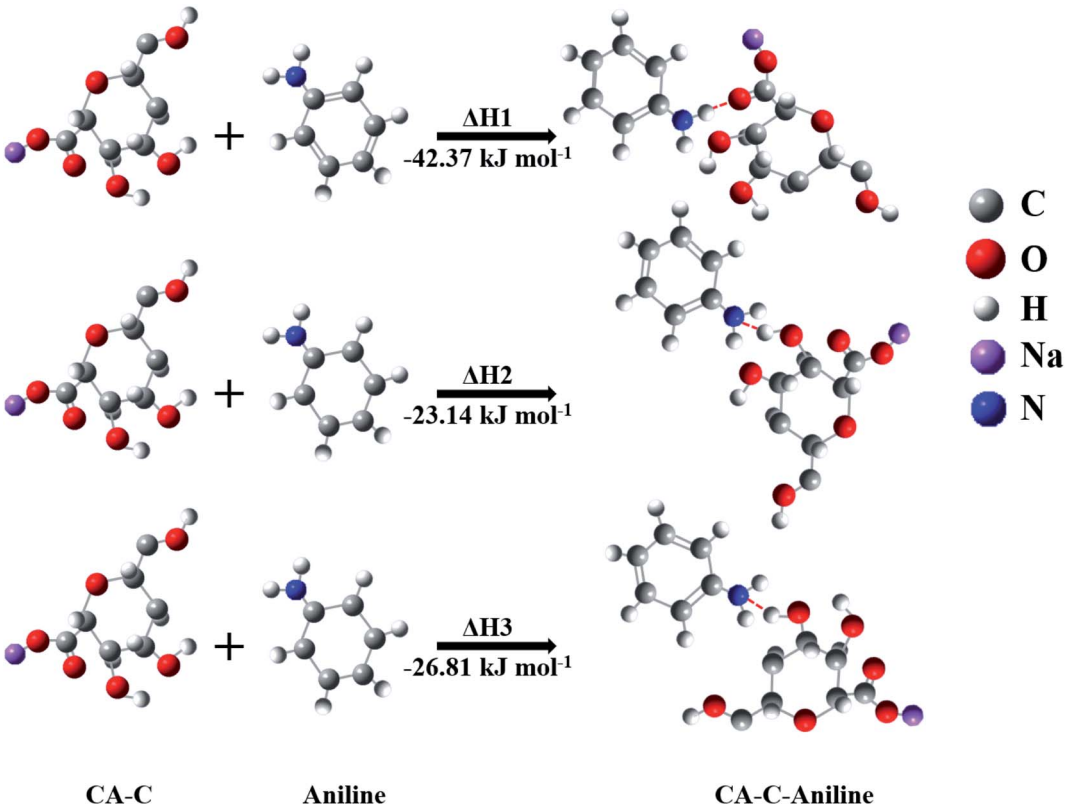

Fig. 8 The Gaussian simulations of hydrogen bonding adsorption between aniline molecules and various groups of the carboxylated cellulose monomer.

ammonia group of aniline *via* hydrogen bond adsorption. The thermodynamic parameters of the above adsorption processes were simulated. As shown in Fig. 8, the enthalpy variation can be extracted to be $\Delta H1 = -42.37$ kJ mol^{-1}, $\Delta H2 = -23.14$ kJ mol^{-1}, and $\Delta H3 = -26.81$ kJ mol^{-1}. According to the adsorption theories, reversible physical adsorption can be qualitative when the ΔH is in the range of -40 to 0 kJ mol^{-1}. A strong chemical reaction can be qualitative when the ΔH is less than -80 kJ mol^{-1}. Weak chemical adsorption can be qualitative when the ΔH is in the range of -80 to -40 kJ mol^{-1}.[28] Based on the simulation results, aniline molecules will interact with the hydroxyl and carboxyl groups after contacting the surface of the carboxylated cellulose aerogel. Meanwhile, the interaction with the carboxyl group belongs to weak chemical adsorption, which plays the most important role in the aniline sensing process.

4. Conclusion

In summary, a carboxylated cellulose aerogel has been developed as a QCM sensing material for rapid aniline detection for the first time. The response and recovery times are as low as 13 s and 8 s, respectively. In the aniline concentration range of 1 to 40 ppm, there is a linear relationship between the response and aniline concentration. The detection limit of the sensor is lower than 1 ppm. Based on the experimental results, the carboxylated cellulose aerogel-loaded sensor shows excellent selectivity. Its repeatability and stability are also favorable. The Gaussian 09 software simulation indicates that the carboxyl group is the most important site for adsorbing aniline molecules. This work supports the development prospect of green cellulose aerogel materials in the field of gas sensors.

Conflicts of interest

The authors declare that they have no known competing financial interests or personal relationships that could have appeared to influence the work reported in this paper.

Acknowledgements

This research was supported by the National Natural Science Foundation of China under Grant No. 62001420, Zhejiang Provincial Natural Science Foundation of China (No. LQ21F010017), and Science Foundation of Zhejiang Gongshang University Hangzhou College of Commerce, Zhejiang Gongshang University, China (ZJHZCC) under Grant No. 2222111.

References

1 Y.-H. Zhang, C.-N. Wang, F.-L. Gong, P. Wang, U. Guharoy, C. Yang, H.-L. Zhang, S.-M. Fang and J. Liu, *J. Hazard. Mater.*, 2020, 388.
2 P. Kovacic and R. Somanathan, *Medchemcomm*, 2011, **2**, 106–112.
3 C. He, Q. He, C. Deng, L. Shi, D. Zhu, Y. Fu, H. Cao and J. Cheng, *Chem. Commun.*, 2010, **46**, 7536–7538.
4 Y. Gui, K. Tian, J. Liu, L. Yang, H. Zhang and Y. Wang, *J. Hazard. Mater.*, 2019, 380.
5 T. Spataru, N. Spataru and A. Fujishima, *Talanta*, 2007, **73**, 404–406.
6 S. M. Majhi, A. Mirzaei, H. W. Kim, S. S. Kim and T. W. Kim, *Nano Energy*, 2021, 79.
7 H. Nazemi, A. Joseph, J. Park and A. Emadi, *Sensors*, 2019, **19**, 1285.
8 F. Fauzi, A. Rianjanu, I. Santoso and K. Triyana, *Sens. Actuators, A*, 2021, 330.
9 L. Wang, *Sens. Actuators, A*, 2020, 307.
10 J. Lin, N. Gao, J. Liu, Z. Hu, H. Fang, X. Tan, H. Li, H. Jiang, H. Liu, T. Shi and G. Liao, *J. Mater. Chem. A*, 2019, **7**, 9068–9077.
11 H. Li, Q. Zheng, J. Luo, Z. Cheng and J. Xu, *Sens. Actuators, B*, 2013, **187**, 604–610.
12 L. Wang, Y. Wu and C. Yu, *J. Solid State Chem.*, 2022, 310.
13 L. Wang, B. Wang, Y. Wu and J. Song, *J. Iran. Chem. Soc.*, 2022, **19**, 211–218.
14 Y. Kosaki, H. Izawa, S. Ishihara, K. Kawakami, M. Sumita, Y. Tateyama, Q. Ji, V. Krishnan, S. Hishita, Y. Yamauchi, J. P. Hill, A. Vinu, S. Shiratori and K. Ariga, *ACS Appl. Mater. Interfaces*, 2013, **5**, 2930–2934.
15 F. Liu, M. Xiao, Y. Ning, S. Zhou, J. He, Y. Lin and Z. Zhang, *Sci. China Inf. Sci.*, 2022, **65**, 162402.
16 G. Gorgolis and C. Galiotis, *2D Materials*, 2017, **4**, 032001.
17 L. Keshavarz, M. R. Ghaani, J. D. MacElroy and N. J. English, *Chem. Eng. J.*, 2021, **412**, 128604.
18 N. L. Torad, S. Zhang, W. A. Amer, M. M. Ayad, M. Kim, J. Kim, B. Ding, X. Zhang, T. Kimura and Y. Yamauchi, *Adv. Mater. Interfaces*, 2019, **6**, 1900849.
19 A. Rianjanu, F. Fauzi, K. Triyana and H. S. Wasisto, *ACS Appl. Nano Mater.*, 2021, **4**, 9957–9975.
20 L. Wang, R. Guo, J. Ren, G. Song, G. Chen, Z. Zhou and Q. Li, *Ceram. Int.*, 2020, **46**, 10362–10369.
21 L. Wang, Z. Wang, Q. Xiang, Y. Chen, Z. Duan and J. Xu, *Sens. Actuators, B*, 2017, **248**, 820–828.
22 D. Yan, P. Xu, Q. Xiang, H. Mou, J. Xu, W. Wen, X. Li and Y. Zhang, *J. Mater. Chem. A*, 2016, **4**, 3487–3493.
23 C. Li, H. Ma, S. Venkateswaran and B. S. Hsiao, *Chem. Eng. J.*, 2020, 389.
24 N. M. Shaalan, M. Rashad and M. A. Abdel-Rahim, *Mater. Sci. Semicond. Process.*, 2016, **56**, 260–264.
25 Z. Kang, D. Zhang, T. Li, X. Liu and X. Song, *Sens. Actuators, B*, 2021, 345.
26 L. Wang, Y. Wu, Z. Pan and C. Yu, *Sens. Actuators, A*, 2022, 333.
27 D. Zhang, Y. Fan, G. Li, W. Du, R. Li, Y. Liu, Z. Cheng and J. Xu, *Sens. Actuators, B*, 2020, 302.
28 P. Xu, H. Yu, S. Guo and X. Li, *Anal. Chem.*, 2014, **86**, 4178–4187.